Influence of Flexoelectric Effect on Director Alignment of Nematic Liquid Crystals in Axial Arrangement Cylindrical Cells

Hong-Hong Liu(刘红红)[1], Yan-Jun Zhang(张艳君)[1,2**], Huai-Rui Yue(岳怀瑞)[1], Li-Zhi Zhu(朱礼智)[3], Rui-Xia Yang(杨瑞霞)[2]

[1]*Department of Physics, Hebei University of Technology, Tianjin 300401*
[2]*School of Electronic and Information Engineering, Hebei University of Technology, Tianjin 300401*
[3]*Department of Wood Science and Technology, Tianjin University of Science and Technology, Tianjin 300222*

(Received 19 October 2017)

A positive nematic liquid crystal (5CB) sample is confined in cylindrical cells under strong or weak axial anchoring boundary conditions when a radial nonuniform low-frequency electric field is applied and the flexoelectric effect is taken into account. Based on the Frank elastic free energy, the surface energy of the Rapini–Papoular approximation, the polarization free energy and the flexoelectric free energy caused by electric field, we obtain the free energy density of the nematic and solve the corresponding Euler–Lagrange equation numerically. We investigate the director distribution, the critical voltage and the critical exponent of nematic liquid crystal in cylindrical cells. It follows that the critical exponent is the classical one. It is also shown that the critical voltage in the system is affected by the flexoelectric effect, the geometric effect and radial weak anchoring effect on the cylindrical surfaces. A new type of director transition caused by the flexoelectric effect, the dielectric coupling effect and the radial weak anchoring effect is found.

PACS: 61.30.Dk, 61.30.Hn, 61.30.Gd DOI: 10.1088/0256-307X/35/2/026103

Distribution of nematic liquid crystals (NLCs) in cylindrical cells has been studied for approximately 50 years since its initial discovery by Meyer *et al.*,[1,2] and has been solved in a special case by Parodi, then discussed by de Gennes and Prost.[3] Subsequently, the same problem was re-examined by Williams[4] considering that the elastic constants of splay and bend are different, in the strong anchoring approximation. The first calculation has been carried out under hard anchoring homeotropic boundary conditions,[5,6] and recently under more arbitrary anchoring boundary conditions researchers have studied the competition between elastic energies and molecular anchoring energies.[7–10] Then, Halevi *et al.* have investigated the orientational transition and a critical value of an axial applied field $\boldsymbol{E}_0$ was given under effects of an applied low-frequency electric field.[11,12] They also illustrated that different $\boldsymbol{E}_0$ can be tuned from the opened to the closed photonic band gap of NLC-infilled photonic crystals. The systems that involve liquid crystal alignment between two concentric cylinders have been investigated in connection with the flexoelectric instability,[13] with the stability analysis of the orientational profile,[14] and the Fréedericskz transition occurring in the absence of external electric field[15] depending on the ratio of the radii of the inner and outer cylinders.[16,17] The flexoelectricity describes the linear coupling between an applied electric field and gradients in the director field.[18] Under the action of applied voltage,[15,19] the director distribution in NLCs between the cylindrical cells is affected by the dielectric coupling effect and the flexoelectric effect.[20,21]

In this Letter, we analyze the order parameter critical exponent, molecular orientation and critical voltage based on the flexoelectric effect in nematics between two coaxial cylinders under strong or weak anchoring boundary conditions. Firstly, the geometry is described. According to the elasticity theory, the fundamental differential equations are obtained under the strong and weak anchoring boundary conditions, which describe the Fréedericskz transition of flexoelectric effect and critical phenomenon of flexoelectric effect. The finite difference iterative method is used for numerical solution, which discusses the influence of flexoelectric effect on the director transitions and the critical voltage.

Let us consider a cell limited by two concentric cylinders filled with positive NLCs whose inner and outer radii are r_1 and r_2, respectively, and $r_2 > r_1$, as can be seen from Fig. 1. The two surfaces of the cylindrical cell are homogeneous and the easy direction is along the axial direction imposed by the inner and outer surfaces. All nematic molecules in cylindrical cell are along the axial alignment. The director reads

$$\boldsymbol{n} = \sin\psi(r)\hat{\boldsymbol{r}} + \cos\psi(r)\hat{\boldsymbol{z}}, \tag{1}$$

where ψ is the angle between $\boldsymbol{n}$ and $\boldsymbol{z}$ in the axial plane. We shall consider the case of applied electric field acting along the radial direction from the inner cylindrical surface to the outer. The radial component of the electric field is

$$\boldsymbol{E} = \frac{V}{r\ln\rho}\hat{\boldsymbol{r}}, \tag{2}$$

**Corresponding author. Email: zyj513@hebut.edu.cn
© 2018 Chinese Physical Society and IOP Publishing Ltd

where $\rho = \frac{r_2}{r_1}$, and $V = V(r_1) - V(r_2)$ is the voltage drop across the cylinders. This model is another case of Ref. [1].

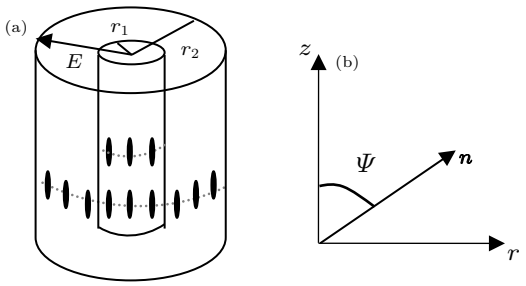

Fig. 1. Nematic sample in geometry formed by two concentrical cylinders and all molecules in axial alignment. (a) The director lies in the axial plane, i.e., the plane parallel to the cylinder axes along z, and (b) a sketch of the coordinates r, z and ψ.

As shown in Fig. 1, the problem is solved under the boundary conditions $\psi(r_1) = \psi(r_2) = 0$, i.e., the molecules are fixed at the surface by considering strong anchoring. Here $f_{\rm elast}$ is Frank's elastic free energy density,[2]

$$f_{\rm elast} = \frac{1}{2}[K_{11}(\nabla\cdot\boldsymbol{n})^2 + K_{22}(\boldsymbol{n}\cdot\nabla\times\boldsymbol{n})^2 + K_{33}(\boldsymbol{n}\times\nabla\times\boldsymbol{n})^2]. \tag{3}$$

The electric free energy $f_{\rm elect}$ is given by

$$f_{\rm elect} = -\frac{\varepsilon_{\rm a}}{2}(\boldsymbol{n}\cdot\boldsymbol{E})^2, \tag{4}$$

where $\varepsilon_{\rm a} = \varepsilon_0\Delta\varepsilon$ is the dielectric constant. In the presence of the electric field, nematic liquid crystals have a positive dielectric anisotropy ($\Delta\varepsilon = \varepsilon_{\parallel} - \varepsilon_{\perp} > 0$), where $\parallel$ and $\perp$ refer to the direction of $\boldsymbol{n}$, and the parameter ε_0 is the dielectric constant in vacuum. The contribution of flexoelectric polarization is described by the Meyer model,[19,22,23]

$$\begin{aligned}\boldsymbol{P} &= e_1\boldsymbol{n}(\nabla\cdot\boldsymbol{n}) + e_3(\nabla\times\boldsymbol{n})\times\boldsymbol{n}\\ &= e_1\Big[\Big(\sin^2\psi\frac{1}{r} + \sin\psi\cos\psi\frac{d\psi}{dr}\Big)\hat{\boldsymbol{r}}\\ &\quad + \Big(\sin\psi\cos\psi\frac{1}{r} + \cos^2\psi\frac{d\psi}{dr}\Big)\hat{\boldsymbol{z}}\Big]\\ &\quad + e_3\Big[\sin\psi\cos\psi\frac{d\psi}{dr}\hat{\boldsymbol{r}} - \sin\psi\frac{d\psi}{dr}\hat{\boldsymbol{z}}\Big].\end{aligned} \tag{5}$$

The flexo-polarization $\boldsymbol{P}$ induces the splay and bend deformations of the director field where e_i ($i = 1$ and 3) denote the flexoelectric coefficients.[20] The flexoelectric free energy can be given by

$$\begin{aligned}f_{\rm fl} &= -(\boldsymbol{E}\cdot\boldsymbol{P})\\ &= -\frac{V}{r\ln\rho}\Big[e_1\Big(\frac{\sin^2\psi}{r} + \sin\psi\cos\psi\frac{d\psi}{dr}\Big)\\ &\quad + e_3\Big(\sin\psi\cos\psi\frac{d\psi}{dr}\Big)\Big].\end{aligned} \tag{6}$$

The total elastic energy density is composed of the Frank expression (in which the twist term as well as the saddle-splay term are absent) with a contribution coming from the dielectric coupling and the flexoelectric effect. Thus the total free energy per unit length, in the limit of small distortion ($\psi \ll 1$), ignoring terms independent of ψ, is given by

$$\begin{aligned}F &= \int_v (f_{\rm elast} + f_{\rm elect} + f_{\rm fl})dv\\ &= \pi K_{11}\int_{r_1}^{r_2} r\Big[\Big(\frac{d\psi}{dr}\Big)^2 - \frac{h}{r^2}\psi^2\Big]dr,\end{aligned} \tag{7}$$

where we have introduced the dimensionless quantities

$$h = -1 + \frac{\varepsilon_{\rm a}V^2}{K_{11}\ln^2\rho} + \frac{2e_1V}{K_{11}\ln\rho}.$$

The transformation $r = r_1e^x$ is brought into Eq. (7) to obtain the simple form

$$F = \pi K_{11}\int_0^{\ln\rho}\Big[\Big(\frac{d\psi}{dx}\Big)^2 - h\psi^2\Big]dx. \tag{8}$$

After minimizing F, with the resulting Euler–Lagrange equation, we obtain

$$\frac{d^2\psi}{dx^2} + h\psi = 0. \tag{9}$$

The solution satisfies the boundary conditions

$$\psi(x) = \psi_{\rm M}\sin\Big(\frac{l\pi}{\ln\rho}x\Big). \tag{10}$$

If $(l\pi/\ln\rho)^2 = h$, for $l = 1, 2, 3, \ldots$, the quantity $\psi_{\rm M}$ will be the maximum amplitude of $\psi(x)$, and in the approximation we are working it can be considered to be very small. It corresponds to the value of ψ in the middle points between the cylindrical surfaces when $l = 1$, i.e., $\psi[(\ln\rho)/2] = \psi_{\rm M}$.

The situation of the lower energy corresponds to $l = 1$. Using the definition of h, we obtain the general expression for the critical voltage in the cylinder geometry,

$$V_{\rm c} = -\frac{e_1\ln\rho}{\varepsilon_{\rm a}} + \sqrt{\frac{e_1^2\ln^2\rho}{\varepsilon_{\rm a}^2} + \frac{K_{11}(\ln^2\rho + \pi^2)}{\varepsilon_{\rm a}}}. \tag{11}$$

This is the critical voltage for the (cylindrical) Fréedericskz transition. If a voltage $V < V_{\rm c}$ is applied, no deformation will appear in the system; if, on the other hand, $V \geq V_{\rm c}$, we can obtain a distorted situation, and the director profile is given by Eq. (11) with $l = 1$.

The complete expression for the free energy can be rewritten as

$$F[\psi(x)] = \pi K_{11}\int_0^{\ln\rho}\Big\{\Big[1 - \sigma^2 + k\Big(\frac{d\psi}{dx}\Big)^2\Big]\sin^2\psi + \Big(\frac{d\psi}{dx}\Big)^2\Big\}dx. \tag{12}$$

The relations are $\sigma^2 = \frac{\varepsilon_a V^2}{K_{11}\ln\rho^2} + \frac{2e_1 V}{K_{11}\ln\rho}$ and $k = \frac{K_{33}}{K_{11}} - 1$, where a constant term is omitted. Minimizing the free energy, after some calculations, we obtain the following differential equation

$$\frac{1}{2}\sin 2\psi\Big[\sigma^2 + k\Big(\frac{d\psi}{dx}\Big)^2 - 1\Big] + (1 + k\sin^2\psi)\frac{d^2\psi}{dx^2} = 0. \tag{13}$$

Using the relations $\psi(x/2) = \psi_M$ and $(d\psi/dx)_{x=\ln\rho/2} = 0$, it is possible to obtain a first integral of Eq. (13), and the function $\psi(x)$ can be given by

$$\int_0^{\psi(x)} \sqrt{\frac{1 + k\sin^2\xi}{\sin^2\psi_M - \sin^2\xi}}\, d\xi = x\sqrt{h}, \tag{14}$$

which, by means of the change of variables $\sin\varphi = \sin\xi/\sin\psi_M$, and integrating from $x = 0$ to $x = \ln\rho/2$, can be rewritten in the form

$$\int_0^{\pi/2} \sqrt{\frac{1 + k\sin^2\psi_M\sin^2\varphi}{1 - \sin^2\psi_M\sin^2\varphi}}\, d\varphi = \frac{\ln\rho}{2}\sqrt{h}. \tag{15}$$

To investigate the behavior of the order parameter in the vicinity of the transition, we expand Eq. (15) in series of ψ_M. By ignoring higher order terms, we gain

$$\frac{\pi}{2} + \frac{\pi}{8}(1+k)\psi_M^2 = \frac{\ln\rho}{2}\sqrt{h}, \tag{16}$$

$$\psi_M = \frac{2}{\sqrt{1+k}}\sqrt{\frac{\ln\rho}{\pi}\sqrt{\frac{\varepsilon_a V^2}{K_{11}\ln\rho^2} + \frac{2e_1 V}{K_{11}\ln\rho}} - 1} - 1. \tag{17}$$

The behavior of ψ_M, when $V \to V_c$, can be well described by

$$\psi_M = \frac{2}{\sqrt{1+k}}\Big\{\frac{2\varepsilon_a}{K_{11}\pi^2}\Big[\frac{e_1^2\ln\rho^2}{\varepsilon_a^2} + \frac{K_{11}(\ln\rho^2 + \pi^2)}{\varepsilon_a}\Big]^{1/2}(V - V_c)\Big\}^{1/2},$$
$$\psi_M \propto (V - V_c)^{1/2}. \tag{18}$$

According to the previous model, the inner and outer surface energies are considered as in the Rapini–Papoular approximation[24–26] under the weak anchoring boundary condition

$$W_{si} = -\frac{W_i}{2}(\boldsymbol{n}_i\cdot\boldsymbol{s}_i)^2 = -\frac{W_i}{2}\cos^2\psi_i, \ (i = 1, 2), \tag{19}$$

where W_i is the anchoring strengths, $\boldsymbol{n}_i$ is the actual nematic directors, and $\boldsymbol{s}_i$ is the easy directions imposed by the surfaces 1 and 2, respectively, assuming $\boldsymbol{s}_i = 0$. According to Eqs. (12) and (19), the total free energy per unit length of the cylinder is written as

$$\begin{aligned}\frac{F}{\pi K_{11}} = \int_0^{\ln\rho} dx\Big\{\Big[\sin^2\psi + \cos^2\psi\Big(\frac{d\psi}{dx}\Big)^2 + k\sin^2\psi\Big(\frac{d\psi}{dx}\Big)^2\Big] - \Big[\frac{\varepsilon_a V^2}{K_{11}\ln^2\rho}\sin^2\psi + \frac{2e_1 V}{K_{11}\ln\rho}\sin^2\psi\Big]\Big\} + \Big[-\frac{(e_1+e_3)V}{2K_{11}\ln\rho}\cos 2\psi + \frac{1}{2}\cos 2\psi - \frac{W_1 r_1}{K_{11}}\cos^2\psi\Big]\delta(x) \\ + \Big[\frac{(e_1+e_3)V}{2K_{11}\ln\rho}\cos 2\psi - \frac{1}{2}\cos 2\psi - \frac{W_2 r_2}{K_{11}}\cos^2\psi\Big]\delta(x - \ln\rho),\end{aligned} \tag{20}$$

where we have introduced the Dirac delta function δ. The fixed orientational configuration $\psi(x)$ is determined by minimizing the complete free energy. After some simple calculations dealing with the resulting Euler–Lagrange equation, one can find that the equilibrium equation in the bulk is the same as Eq. (13) obtained by strong anchoring. Here $\psi(x)$ satisfy the following weak anchoring boundary conditions on the cylinder's walls at r_1 and r_2, respectively,

$$2(k\sin^2\psi_{r_1} + \cos^2\psi_{r_1})\frac{d\psi}{dx}\Big|_{x=0} - \Big[\frac{W_1 r_1}{K_{11}} + \frac{(e_1+e_3)V}{K_{11}\ln\rho} - 1\Big]\sin 2\psi_{r_1} = 0, \tag{21}$$

$$2(k\sin^2\psi_{r_2} + \cos^2\psi_{r_2})\frac{d\psi}{dx}\Big|_{x=\ln\rho} + \Big[\frac{W_2 r_2}{K_{11}} - \frac{(e_1+e_3)V}{K_{11}\ln\rho} + 1\Big]\sin 2\psi_{r_2} = 0. \tag{22}$$

In the following we will use the specific case 5CB liquid crystal. The material parameters used are[27] $K_{11} = 1.2\times10^{-11}$ N, $K_{33} = 1.5792\times10^{-11}$ N, $e_1 = -6.9\times10^{-11}$ C/m, $e_3 = -4.5\times10^{-11}$ C/m, $\Delta\varepsilon = 13.3$, and $\varepsilon_0 = 8.854\times10^{-12}$ C^2/(N·m^2). Equations (9), (13), (17), (21) and (22) are calculated using the finite-difference iterative method, and the director distribution of the system is obtained by computer simulation.

Figures 2(a) and 2(b) are the curves of orientation distribution when the surfaces take the strong anchoring conditions. The director orientation is non-monotonous in cylindrical cells and the values of ψ first increase and then decrease. From the comparison of Figs. 2(a) and 2(b), we can see that the bifurcation of Fig. 2(a) is steeper at the same voltage. Thus the critical voltage value of the axial arrangement model is larger by considering the flexoelectric effect. As is the theoretical result obtained by Eq. (11), the critical voltages are $V_c = 1.5432$ V and $V_c = 1.0270$ V, respectively, considering the flexoelectric effect and ignoring the flexoelectric effect. Due to the flexoelectric effect and the geometrical effect, the critical voltage of the system is larger than the only influence of dielectric

coupling in the vicinity of the transition. According to Eq. (5), some bulk terms have been added to the expression of $\boldsymbol{P}$ for the geometrical effect. It is indicated that the flexoelectric effect and the dielectric coupling effect influence the distribution of liquid crystal director in cylindrical cells at the same time and their effects are opposite.

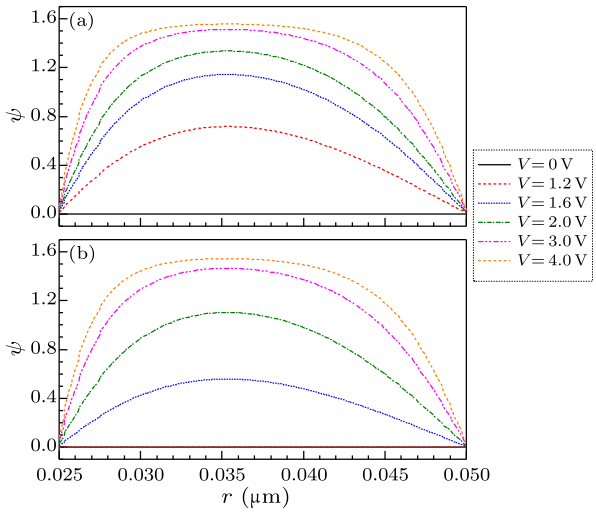

Fig. 2. Director configuration ψ versus r for 5CB with $r_1 = 0.025\,\mu$m, $r_2 = 0.05\,\mu$m and radial electric field for different values of V. (a) Flexoelectric effect is absent. (b) Flexoelectric effect is considered.

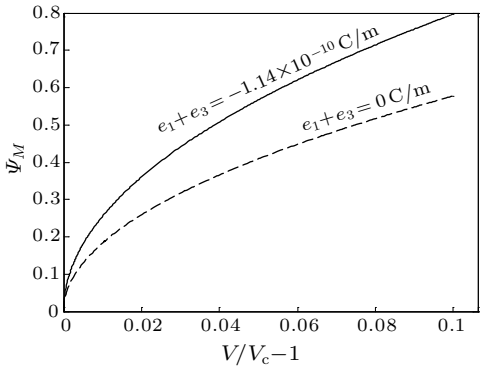

Fig. 3. Dependence of $\psi_{\rm M}$ on $(V/V_{\rm c}-1)$ for $r_1 = 0.025\,\mu$m and $r_2 = 0.05\,\mu$m when the surfaces take strong anchoring conditions by considering the flexoelectric effect and ignoring the flexoelectric effect.

Figure 3 is a distribution curve of the maximum value of the director angle in the cylindrical cell with the voltage change. If the maximum value of the tilt angle is assumed to be an order parameter, its behavior of the transition can be used to obtain the critical exponent. It follows that the critical exponent is also the classical one ($\beta = 1/2$)[1] by considering the flexoelectric effect and ignoring the flexoelectric effect. The critical exponent is the same as the one in electric field theory and accounts for the usual behavior of the order parameter in the Fréedericskz transition in a hybrid cell when a planar geometry is considered.[28]

Figure 4(a) is a curve of orientation distribution when the flexoelectric effect is ignored. Under the influence of the radial weak anchoring effect of cylindrical surface and the electric field, the director orientation slightly decreases but is close to the same from the inside to the outside with the same voltage, which shows the outer surface anchoring energy slightly stronger for the same anchoring energy, because the number of outer surface molecules is greater than the number of inner surface molecules.[29] As the voltage increases, the value of the director angle is gradually increased, which is the result of the electric field effect enhancing. Here the saturation voltage is defined as the critical value of the radially applied electric field when the director alignment is perpendicular to the axial direction in the axial plane.[2] When the voltage is greater than $V = 0.4$ V, the nematic liquid crystal does not deform along the radial direction. It shows that the system's saturation voltage is about $V_{\rm s} = 0.4$ V.

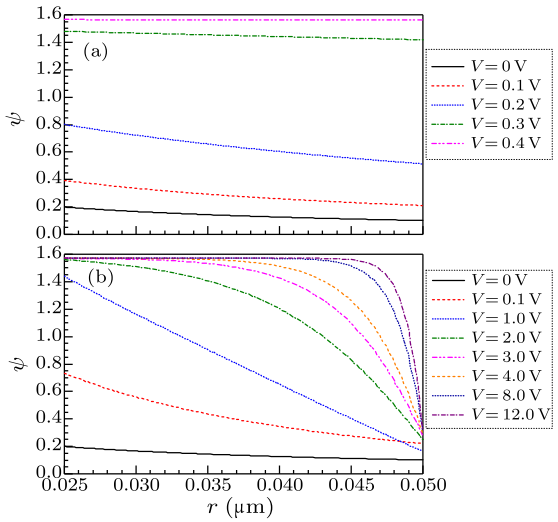

Fig. 4. Director configurations ψ versus r, for 5CB with $W_i/K_{11} = 6.0 \times 10^4\,{\rm m}^{-1}$, $r_1 = 0.025\,\mu$m and $r_2 = 0.05\,\mu$m. (a) Flexoelectric effect is absent. (b) Flexoelectric effect is considered.

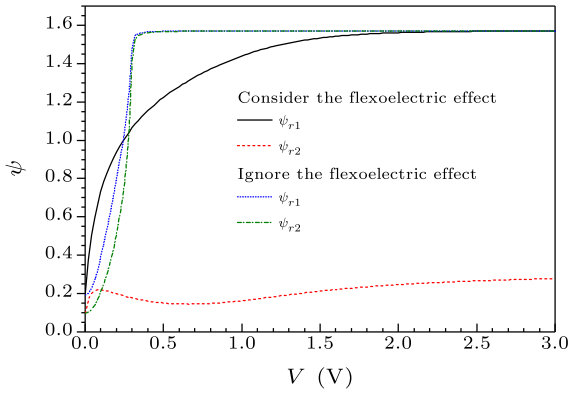

Fig. 5. Director configurations ψ_{r_1} and ψ_{r_2} on the cylinder's walls at r_1 and r_2 versus V, for 5CB with $W_i/K_{11} = 6.0 \times 10^4\,{\rm m}^{-1}$, $r_1 = 0.025\,\mu$m, and $r_2 = 0.05\,\mu$m.

The director distribution is shown in Fig. 4(b)

when the flexoelectric effect caused by electric field is considered. According to the equilibrium Eq. (13) and the parameter σ^2, the dielectric coupling effect term and the flexoelectric effect term are calculated to be equal when the voltage is about 0.8 V. For the voltage less than 0.8 V, the flexoelectric effect is stronger than the dielectric coupling effect. The flexoelectric effect and the dielectric coupling effect in the bulk influence the distribution of liquid crystal director in cylindrical cells at the same time and their effects are opposite. According to the boundary condition Eqs. (21) and (22), the flexoelectric effect and the anchoring effect on the inner surface influence the distribution of the inner surface molecules at the same time and their effects are the same to promote the radial reorientation of the inner surface molecules. The flexoelectric effect on the outer surface is equivalent to the anchoring effect on the outer surface about 0.2 mV. For a voltage greater than 0.2 mV, the outer surface flexoelectric effect is greater than the surface anchoring effect. The flexoelectric effect and the anchoring effect on the outer surface influence the distribution of the outer surface molecules at the same time and their effects promote the axial effect of the molecules on the outer surface. According to Figs. 4(b) and 5, the director orientation considering the flexoelectric effect is no longer consistent with the increasing voltage. The closer the inner surface is, the larger the director angle is. The director angle of the closer to the outer surface is smaller. There is no saturation voltage for the influence of the flexoelectric effect in the model of the axial arrangement. However, with the increase of the voltage, the director forms a hybrid arrangement. It is indicated that the flexoelectric effect and the surface anchoring effect enhance the radial effect of the molecules on the inner surface and enhance the axial effect of the molecules on the outer surface. Therefore, a new type of director transition caused by the flexoelectric effect, the dielectric coupling effect and the surface anchoring effect is found.

In summary, we have calculated the nano concentric tube configurations of nematic liquid crystal confined between two coaxial cylinders submitted to a low-frequency electric field with arbitrary anchoring boundary conditions for director transition. The influence of the flexoelectric effect on the director's deformation is studied under the action of the electric field. According to the differential equation and computer numerical simulation, the results show that: (1) the critical exponents of the director's deformation are both $\beta = 1/2$ regardless of considering the flexoelectric effect or ignoring the flexoelectric effect, which is consistent with the results in the mean field theory. (2) Under strong anchoring boundary conditions, the flexoelectric effect makes the critical voltage of the axial arrangement model larger. Thus the dielectric coupling effect and the flexoelectric effect influence liquid crystal director transitions at the same time, and their effects are opposite. (3) Under weak anchoring boundary conditions, the influence of the flexoelectric effect makes the model of the axial arrangement without saturation voltage, but with the increase of the voltage to form a hybrid arrangement. (4) Under weak anchoring boundary conditions, the flexoelectric effect and the surface anchoring effect enhance the radial effect of the molecules on the inner surface and the axial effect of the molecules on the outer surface. (5) Under weak anchoring boundary conditions, a new type of director transition caused by the flexoelectric effect, the dielectric coupling effect and the surface anchoring effect is found.

References

[1] Souza R T D, Dias J C and Mendes R S et al 2010 *Physica* A **389** 945
[2] Corellamadueño A, Castellanosmoreno A, Gutiérrezlópez S et al 2008 *Phys. Rev.* E **78** 022701
[3] De Gennes P G and Prost J 1993 *The Physics of Liquid Crystals* (Oxford: Oxford University Press)
[4] Williams D R M 1994 *Phys. Rev.* E **50** 1686
[5] Heuer H, Kneppe H and Schneider F 1991 *Liq. Cryst.* **200** 51
[6] Cladis P E and Kléman M 1972 *J. Phys.* **33** 591
[7] Allender D W, Crawford G P and Doane J W 1991 *Phys. Rev. Lett.* **67** 1442
[8] Crawford G P, Allender D W and Doane J W 1992 *Phys. Rev.* A **45** 8693
[9] Kralj S and Zumer S 1995 *Phys. Rev.* E **51** 366
[10] Burylov S V 1997 *J. Exp. Theor. Phys.* **85** 873
[11] Chen S and Wei J 1994 *J. Appl. Phys.* **75** 2799
[12] Halevi P, Reyes-Avendaño J A and Reyes-Cervantes J A 2006 *Phys. Rev.* E **73** 040701
[13] Kotov I V, Khazimullin M V and Krekhov A P 2001 *Mol. Cryst. Liq. Cryst.* **366** 885
[14] Tsuru H and Wadati M 1984 *J. Phys. Soc. Jpn.* **53** 2908
[15] Williams D R and Halperin A 1993 *Phys. Rev.* E **48** R2366
[16] Carlsson T, Stewart I W and Leslie F M 1991 *Liq. Cryst.* **9** 661
[17] Williams C E, Cladis P E and Kleman M 1973 *Mol. Cryst. Liq. Cryst.* **21** 355
[18] Meyer R B 1969 *Phys. Rev. Lett.* **22** 918
[19] Aoki N, Ohki Y and Yahagi K 1979 *Jpn. J. Appl. Phys.* **18** 523
[20] Alexe-Ionescu A L, Barbero G and Petrov A G 1993 *Phys. Rev.* E **48** R1631
[21] Wang Q 2001 *Acta Sin. Phys.* **50** 931 (in Chinese)
[22] Song H W, Ye W J, Zhang Z D et al 2016 *Chin. Phys.* B **25** 036101
[23] Ye W J, Xing H Y, Cui W J et al 2014 *Chin. Phys.* B **23** 116101
[24] Pizzirusso A, Berardi R, Muccioli L et al 2012 *Chem. Sci.* **3** 573
[25] Rapini A and Papoular M 1969 *J. Phys. Paris.* C **30** C4-54
[26] Xing H Y, An Y S, Wang M Y et al 2015 *Acta Phys. Sin.* **64** 194206 (in Chinese)
[27] Takahashi T, Hashidate S, Nishijou H et al 1998 *Jpn. J. Appl. Phys.* **37** 1865
[28] Barbero G and Evangelista L R 2001 *An Elementary Course on the Continuum Theory for Nematic Liquid Crystals* (Singapore: World Scientific)
[29] Liu H H and Zhang Y J 2017 *Chin. J. Liq. Cryst. Disp.* **32** 13